

ASY-EOS experiment at GSI

P. RUSSOTTO^{1,2}, L. ACOSTA¹, M. ADAMCZYK³, A. AL-AJLAN⁴,
M. AL-GARAWI⁵, S. AL-HOMAIDHI⁴, F. AMORINI¹, L. AUDITORE^{6,7},
T. AUMANN⁸, Y. AYYAD⁹, V. BARAN^{1,29}, Z. BASRAK¹⁰, J. BENLLIURE⁹,
C. BOIANO¹¹, M. BOISJOLI¹², K. BORETZKY¹³, J. BRZYCHCZYK³,
A. BUDZANOWSKI¹⁴, G. CARDELLA¹⁵, P. CAMMARATA¹⁶,
S. CAVALLARO^{15,2}, Z. CHAJECKI¹⁷, M. CHARTIER¹⁸, A. CHBIHI¹²,
M. COLONNA¹, B. CZECH¹⁴, E. DE FILIPPO¹⁵, M. DI TORO^{1,2},
M. FAMIANO¹⁹, A. LE FEVRE¹³, I. GAŠPARIĆ¹⁰, E. GERACI^{15,2},
L. GRASSI¹⁰, V. GRECO^{1,2}, C. GUAZZONI^{11,20}, P. GUAZZONI^{11,21},
M. HEIL¹³, L. HEILBORN¹⁶, R. INTROZZI²², T. ISOBE²³, K. KEZZAR⁵,
M. KIŠ^{13,10}, S. KUPNY³, N. KURZ¹³, E. LA GUIDARA¹⁵,
G. LANZALONE^{1,24}, P. LASKO³, Y. LEIFELS¹³, R. LEMMON²⁵, Q. LI²⁶,
I. LOMBARDO^{27,28}, D. LORIA^{6,7}, J. LUKASIK¹⁴, W.G. LYNCH¹⁷,
P. MARINI¹⁶, Z. MATTHEWS¹⁸, L. MAY¹⁶, T. MINNITI^{6,7},
M. MOSTAZO⁹, A. PAGANO¹⁵, M. PAPA¹⁵, P. PAWLOWSKI¹⁴,
M. PETROVICI²⁹, S. PIRRONE¹⁵, G. POLITI^{15,5}, F. PORTO^{1,2},
R. REIFARTH¹³, W. REISDORF¹³, F. RICCIO^{11,21}, F. RIZZO^{1,2},
E. ROSATO^{27,28}, D. ROSSI¹³, S. SANTORO^{6,7}, H. SIMON¹³,
I. SKWIRCYNSKA¹⁴, Z. SOSIN³, W. TRAUTMANN¹³, A. TRIFIRÒ^{6,7},
M. TRIMARCHI^{6,7}, B. TSANG¹⁷, M. VESELSKY³⁰, G. VERDE¹⁵,
M. VIGILANTE^{27,28}, A. WIELOCH³, P. WIGG¹⁸, J. WILCZYNSKI³¹,
H.H. WOLTER³², P. WU¹⁸, S. YENNELLO¹⁶, P. ZAMBON^{11,20},
L. ZETTA^{11,21} and M. ZORIC¹⁰

- ¹INFN-LNS, Catania, Italy
²University of Catania, Italy
³Jagiellonian University, Kraków, Poland
⁴KACST, Riyadh, Saudi Arabia
⁵King Saud University, Riyadh, Saudi Arabia
⁶INFN, Sezione di Messina, Italy
⁷University of Messina, Italy
⁸Technische Universität, Darmstadt, Germany
⁹University of Santiago de Compostela, Spain
¹⁰RBI, Zagreb, Croatia
¹¹INFN, Sezione di Milano, Italy
¹²GANIL, Caen, France
¹³GSI, Darmstadt, Germany
¹⁴IFJ-PAN, Krakow, Poland
¹⁵INFN, Sezione di Catania, Italy
¹⁶Texas A&M University, College Station, TX, USA
¹⁷NSCL Michigan State University, MI, USA
¹⁸University of Liverpool, UK
¹⁹Western Michigan University, MI, USA
²⁰Politecnico di Milano, Italy
²¹University degli Studi di Milano, Italy
²²INFN, Politecnico di Torino, Italy
²³RIKEN, Wako, Japan
²⁴Kore University of Enna, Italy
²⁵STFC Daresbury Laboratory, UK
²⁶Huzhou Teachers College, China
²⁷INFN, Sezione di Napoli, Italy
²⁸University of Napoli, Italy
²⁹NIPNE, Bucharest, Romania
³⁰Institute of Physics, Slovak Academy of Sciences Bratislava, Slovakia
³¹INS, Warsaw, Poland
³²LMU, München, Germany

Abstract

The elliptic-flow ratio of neutrons with respect to protons in reactions of neutron rich Heavy-Ion at intermediate energies has been recently proposed as an observable sensitive to the strength of the symmetry term in the nuclear equation of state (EOS) at supra-saturation

densities. The recent results obtained from the existing FOPI/LAND data for $^{197}\text{Au}+^{197}\text{Au}$ collisions at 400 MeV/nucleon in comparison with the UrQMD model allowed a first estimate of the symmetry term of the EOS but suffer from a considerable statistical uncertainty. In order to obtain an improved data set for Au+Au collisions and to extend the study to other systems, a new experiment was carried out at the GSI laboratory by the ASY-EOS collaboration in May 2011.

1 Introduction

In May 2011 the data taking of experiment S394 at GSI has been completed. The symmetric collision systems $^{197}\text{Au}+^{197}\text{Au}$, $^{96}\text{Zr}+^{96}\text{Zr}$ and $^{96}\text{Ru}+^{96}\text{Ru}$ at 400 MeV/nucleon incident energies have been measured. The main aim of the experiment is to measure the ratio of parameters describing the elliptic-flow of neutrons and hydrogen isotopes in Heavy-Ion collisions at relativistic energies in order to obtain constraints on the behavior of the symmetry term of the nuclear equation of state (EOS) at supra-saturation densities [1]. Recently, an estimate of the high density behavior of the symmetry energy has been obtained from the re-analysis of the existing FOPI/LAND data for $^{197}\text{Au}+^{197}\text{Au}$ collisions at 400 MeV/nucleon. Comparison with predictions of the UrQMD transport model [2] favors a density dependence of the potential symmetry term proportional to $(\rho/\rho_0)^\gamma$ with $\gamma = 0.9 \pm 0.4$ [3]. The sensitivity of the proton-neutron elliptic flow difference to the symmetry energy has been more recently confirmed by calculations with the Tübingen version of the QMD transport model [4]. Moreover better data would be important to study isospin effects on the momentum dependence of the in-medium interactions [5]. With the new experiment (S394), an attempt is being made to considerably improve the previous set of data, by improving the statistical accuracy of the measured flow parameters for Au+Au reactions and to extend the flow measurements to other systems. Indeed the study of isospin effects can be improved using new observable like the one related to light fragments up to atomic number of about $Z=4$, with special emphasis on the light isobar pairs $^3\text{H}/^3\text{He}$ and $^7\text{Li}/^7\text{Be}$.

2 Experimental set-up

The Large Area Neutron Detector (LAND) [6], recently upgraded with new TACQUILA GSI-ASIC electronics, was positioned at laboratory angles around 45° with respect to the beam direction, at a distance of about 5 m from the target. A veto-wall of plastic scintillators in front of LAND allows

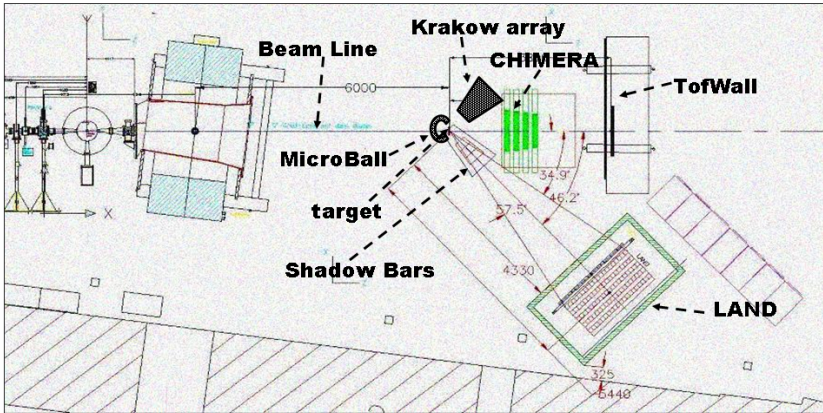


Figure 1: Schematic view of experimental setup.

discrimination of neutrons and charged particles. In such a way it is possible to measure the direct and elliptic collective flows of neutrons and hydrogen isotope at mid-rapidity with high precision in the same angular acceptance. In addition, the Kraków triple-telescope array [7], covering polar angles between 20° and 64° at a distance of 40 cm from the target, permitted the acquisition of data upon yield and collective flows of light charged particles, up to $Z \sim 5$, at mid-rapidity. The determination of impact parameter and the orientation of the reaction plane required the use of several devices: i) the ALADIN Time-of-Flight plastic wall [8] was used to detect forward emitted charged particles at polar angles smaller than 7° ; two walls (front and rear) of $2.5 \times 100 \text{ cm}^2$ plastic scintillators gave information on emission angle, atomic number and velocity of ions; ii) 50 thin CsI(Tl) elements arranged in 4 rings of the Washington-University μ -ball array [9], covering polar angles between 60° and 147° , surrounded the target with the aim of measuring the distribution of backward emitted particles and to discriminate against background reactions on non-target material; iii) 352 CsI(Tl), 12 cm thick, scintillators of the CHIMERA multidetector [10], arranged in 8 rings in 2π azimuthal coverage around the beam axis, covered polar angles between 7° and 20° , measuring the light charged particles. In addition thin ($300 \mu\text{m}$) Silicon detector were placed in front of 32 (4 by ring) CsI detectors in the usual ΔE -E configuration. The beam was guided in vacuum to about 2 m upstream from the target. A thin plastic foil read by two Photo-multipliers was used to tag in time the beam arrival and acted as a start detector for time of flight measurement. A schematic view of the experimental set-up is

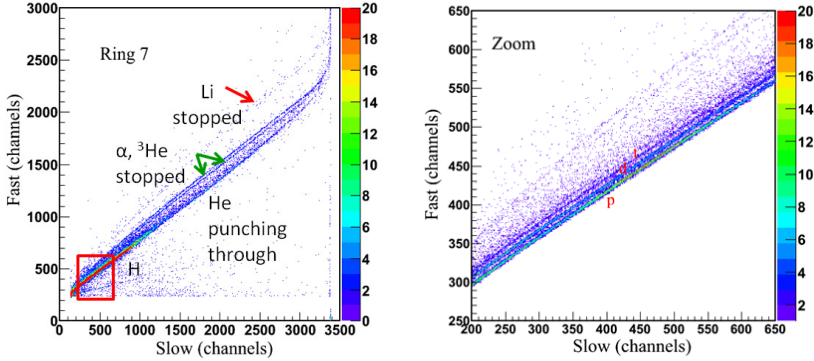


Figure 2: left panel: Fast-vs-Slow component scatter plot as obtained with a CHIMERA CsI(Tl) scintillator placed at a polar angle $\theta_{lab} \sim 17^\circ$ for Au+Au reactions at 400 MeV/nucleon; lines of particles stopped and passing through CsI detector are indicated by arrows; the region highlighted by the square is zoomed on the right panel, showing (from bottom) lines of H punching through, ^1H stopped, ^2H stopped and ^3H stopped .

given in Fig. 1. With beam intensities of about 10^5 pps and targets of 1-2% interaction probability, about $5 * 10^6$ events for each system were collected. Special runs were performed with and without target, in order to measure the background from interaction of projectile ions with air, and with iron shadow bars covering the angular acceptance of LAND in order to measure neutron background. Data acquisition was performed using the MBS data acquisition system available at GSI [11]; the CHIMERA data acquisition was integrated into the MBS system using the time-stamping technique for data synchronization. The analysis of the collected data has been started with calibrations of the individual detector systems and with overall quality checks, and is currently in progress. At the present stage we will report here only on some preliminary results from CHIMERA data.

3 CHIMERA preliminary results and outlook

Identification of Light Charged Particles in CHIMERA CsI(Tl) has been performed using Pulse Shape Analysis based on standard fast-slow techniques; an example is shown in Fig. 2. We have obtained isotopic identification for p,d,t and $^3,4\text{He}$ ions stopped in the CsI detectors. Particles punching through the CsI(Tl) can be separated and identified (only in atomic number) by particles stopped in the scintillators; in fact the difference in ionization

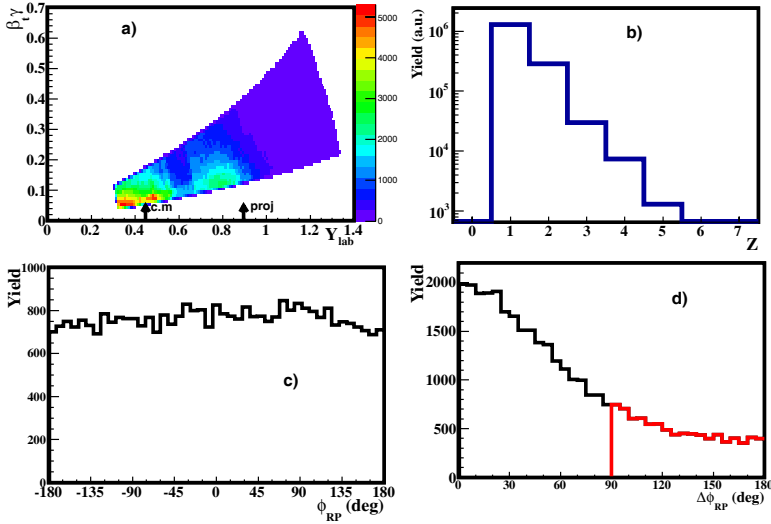


Figure 3: CHIMERA data for Au+Au system; a) transverse velocity versus rapidity in lab reference system ; b) charge distribution; c) orientation of reaction plane obtained using Q-vector method ; d) difference of orientations of reaction plane as obtained using sub-events mixing technique.

densities dE/dx between stopped and punching through ions results in a different fast/slow ratio. At the lowest fast and slow values, an intense ridge due to gamma, fast electrons, and background reactions on non-target material is found. For particles heavier than helium, the slow component is partially saturated, since the gate width for the CsI slow component has been chosen in order to compromise between a good separation of hydrogen isotopes and identification of Li/Be ions within the codifier's maximum energy range. The identification in CsI has been cross-checked with the one obtained in the 32 Si-CsI telescopes via ΔE -E technique. In addition, a digital acquisition sampling technique (14 bit, 50 MHz sampling) was used, in parallel to the standard analog one, in about 10 % of the detectors. Cross checking of identification between standard analog and digital technique has been of fundamental importance; more results are given in [12]. Energy calibration of the fast component has been performed via the evaluation of the punching through points. For particles punching through the detectors, the total kinetic energy has been evaluated from the measured ΔE using energy loss tables. As a global result we show in panel a) of Fig. 3 the transverse velocity versus rapidity in the lab reference system for the Au+Au system.

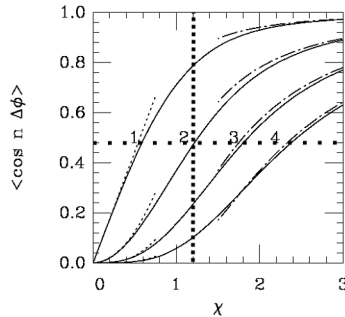


Figure 4: Correction curves for the first four harmonics v_n ($n=1-4$) of the azimuthal distribution as a function of the resolution parameter χ . The obtained $\chi \sim 1.2$ (dashed vertical line) implies a correction factor $\langle \cos(2\Delta\phi) \rangle \sim 0.48$ for the elliptic flow parameter v_2 (dotted horizontal line); picture adapted from [15].

In order to reject fast electrons and background, a threshold of $E/A > 50$ MeV/nucleon has been imposed. In the figure we can clearly see population of two intense regions around mid-rapidity and projectile rapidity; panel b) shows the obtained charge distribution.

An important parameter is the resolution achieved in determining the azimuthal orientation of the reaction plane. It largely determines the uncertainty associated with the determined flow parameters [13]. As a first test we have estimated the reaction plane orientation for events with total charged particle multiplicity $M \geq 10$ in CHIMERA, using the Q-vector method of Ref. [14]. In order to reject the mid-rapidity region, a cut on laboratory rapidity $y > 0.548$ (corresponding to $y > 0.1$ in c.m. system) was used. The obtained reaction plane distribution for a CHIMERA data sample from the $^{197}\text{Au} + ^{197}\text{Au}$ data set is shown in panel c) of Fig. 3; the flatness indicates that the particle angular distributions have not been biased by the event triggering in the experiment. We also tested the resolution achieved in reconstructing the reaction plane using the sub-event mixing technique of Ref. [15]. The distribution of the difference between the two reaction plane orientations extracted by the sub-events is reported in panel d) of Fig. 3. Using the method of [15] we obtain a reaction plane dispersion parameter $\chi \sim 1.2$, resulting in an attenuation of the elliptic flow measurement of ~ 0.5 , as illustrated in Fig. 4, showing correction factors for the Fourier parameters of the azimuthal distribution v_n of order n as a function of χ . The analysis performed so far shows that the particle identification achieved with

the CHIMERA detector modules is better than the one estimated in experimental setup simulations. It is to be expected that these values will improve considerably as soon as the information collected with the Time-of-Flight wall and μ -ball can be included in the analysis.

Work supported by EU under contract No. FP7-25431 (Hadron-Physics2).

References

- [1] B.A. Li et al., Phys. Rep. 464 (2008) 113; V. Baran et al., Phys. Rep. 410 (2005), 335.
- [2] Q. Li et al. Phys. Rev. C 83 044617 (2011) and refs. therein.
- [3] P. Russotto et al., Phys. Lett. B 697 (2011) 471.
- [4] M.D. Cozma, Phys. Lett. B 700 (2011) 139.
- [5] V. Giordano et al. Phys.Rev.C81(2011) 044611.
- [6] Th. Blaich et al., NIM A 314 (1992) 136.
- [7] J. Lukasik et al., see contribution to this volume.
- [8] A. Schüttauf et al., Nucl. Phys. A 607 (1996) 457.
- [9] D.G. Sarantites et al., Nucl. Instr. and Meth. 381 (1996) 418.
- [10] A. Pagano et al., Nucl. Phys. A 734 (2004) 504.
- [11] <http://www-win.gsi.de/daq>.
- [12] L. Acosta et al., 2011 IEEE Nucl. Scie. Symp. Conf. Rec. (2011) 202.
- [13] A. Andronic et al., Eur. Phys. J. A 30 (2008) 31.
- [14] P. Danielewicz et al., Phys. Lett. B 157 (1985) 146.
- [15] J.-Y. Ollitrault, preprint nucl-ex/971003.